DESIGN OF VISCOELASTIC IMPACT ABSORBERS: OPTIMAL MATERIAL PROPERTIES

C. P. CHEN and R. S. LAKES

Departments of Mechanical Engineering and Biomedical Engineering, University of Iowa, Iowa City, IA 52242, U.S.A.

Abstract—Analytical investigations of impact absorption of linear and isothermal viscoelastic materials are described. Three methods based on different considerations and approximations are studied, and similarities are shown in their results. For a viscoelastic buffer of a given thickness, the optimal loss tangent is determined to be approximately one. Greater reductions in impact force can be achieved if the high loss is accompanied by stiffness reduced by a factor of three to four compared with that of an elastic buffer. If the impactor is spherical rather than flat, a higher loss tangent, of the order of 10, is needed to minimize the impact force. A more sophisticated interpretation scheme for the ball rebound test for screening the loss tangent of viscoelastic materials is derived.

NOMENCLATURE

m	the mass of the impactor or indenter
$U(t)$	the displacement of the mass m or indenter
$F(t)$	the impact force
t	time
U_{max}	the maximum displacement of the mass m or indenter
F_{max}	the maximum impact force
E	the axial modulus of the one-dimensional elastic buffer
b, c	cross-section dimensions of the one-dimensional buffer
h	the axial length of the one-dimensional buffer
V	the initial velocity of m
A, θ	amplitude and phase constants, respectively
ω_0	$\sqrt{(Ebc/mh)}$ or $\sqrt{(E'(i\omega)bc/mh)}$
ε	the maximum compressive engineering strain of the one-dimensional buffer
$F_{ext}(t)$	the external force of the forced oscillation of m, $F_{ext}(t) = F_0 \sin(\omega t)$
ω	the angular frequency of harmonic oscillation
ρ	the mass density of the one-dimensional buffer
$E^*(i\omega)$	the uniaxial complex modulus of the one-dimensional buffer, $E^*(i\omega) = E'(i\omega)[1+i \tan \delta]$
$E'(i\omega)$	the axial storage modulus
$\tan \delta$	the loss tangent
Ω^*	$\sqrt{(\rho\omega^2 h^2/E^*(i\omega))}$
α	$(1+\tan \delta^2)^{1/4} \sin(\delta/2)$
β	$(1+\tan \delta^2)^{1/4} \cos(\delta/2)$
t_{cont}	time in which m contacts the buffer
H_0	the height from which the ball is dropped for the rebound test
V_1	the velocity with which the ball rebounds
H_1	the height to which the ball rebounds back
$E(t)$	the relaxation function of a three-element Maxwell model, $E(t) = E_0 + E_1 e^{-t/t_1}$
$[U(s)]$	the Laplace transformation form of $U(t)$
$\alpha_1, \beta_1, k_1, k_2, k_3, k_4, k_5, k_6, k_7, z_0, z_1, z_2$	constants obtained by performing the inverse transformation of $[U(s)]$
R	radius of the rigid sphere
G	the relaxation function in shear of the elastic half-space
$G(t)$	the relaxation function in shear of the viscoelastic half-space, $G(t) = G_0 + G_1 e^{-t/t_1}$
$G'(i\omega)$	the storage modulus in shear
$J(t)$	the creep function in shear of the viscoelastic half-space, $J(t) = 1/G_0 - J_1 e^{-t/t_2}$
J_1	$G_1/(G_0(G_0+G_1))$
t_2	$G_0/(t_1(G_0+G_1))$
v	Poisson's ratio
$r(t)$	the radius of the contact area between the rigid sphere and the viscoelastic half-space
t_m	the time both $U(t)$ and $r(t)$ reach the maximum values
$t_r(t)$	$r(t_r(t)) = r(t)$ for $0 \leqslant t_r(t) \leqslant t_m$, and $t_m < t$
H	mesh width of the Euler method
$\tan \delta^2$	$(\tan \delta)^2$.

INTRODUCTION

The major applications of viscoelastic materials make use of their energy absorption characteristics. The most common usage of these materials is in structures to damp unwanted

acoustic or mechanical vibrations, to avoid environmental noise or vibration-induced failure. Another use of viscoelastic materials is to reduce the impact force of incident mass upon a buffer through the energy absorption characteristics. Viscoelastic polyurethanes have been used as shock-absorbing inner soles for athletic shoes. Material properties in the frequency range 1–100 Hz are relevant in this application. It has been suggested by Light et al. (1980) and Voloshin and Wosk (1982) that shock-absorbing footwear may alleviate symptoms of clinically degenerative joints. For the impact problem, both the frequency characteristics and the transient characteristics of the viscoelastic materials are significant. Attention must be given to the boundary contact condition and the relation between elasticity and viscoelasticity. So far, most of the contact problems of elasticity and visco-elasticity are related to the boundary condition problem, time-independent for elasticity and time-dependent for viscoelasticity. Some results in this area are used to interpret the ball rebound test to determine the loss tangent of viscoelastic materials. Measurements of the coefficient of restitution of steel balls on plates of glass and plastics were made by Tillett (1954) and found to be a function of the specimen's viscoelastic properties. The coefficient of restitution obtained experimentally was in agreement with that calculated from Zener's formulae (1941). Pao (1955) extended the Hertz theory of impact to the viscoelastic case. Numerical calculations were carried out for some particular materials whose actual spectra were replaced with more convenient line spectra. Flom (1960) presented the ball rebound method, in which he measured the rebound height and time of impact of polymeric speci-mens, from which the loss tangent and the equivalent frequency were reduced, as a special case of ball free vibration. The penetration of a viscoelastic half-space by a rigid spherical indenter was investigated by Hunter (1960) in a quasi-static approximation. The duration of contact and coefficient of restitution can therefore be estimated for "glass-like" materials. Using data obtained from free torsional vibration experiments, the impact of a rigid sphere onto a viscoelastic half-space was solved numerically by Calvit (1967). The rebound of a steel ball from a block of polymer was therefore predicted for various temperatures. However, no design aspects were emphasized by the authors mentioned above. Selection of viscoelastic materials for impact absorption on the basis of their loss tangent still seems to be beyond the research works available so far.

The objectives of the present analysis are to determine the optimal loss tangent for impact absorption and to arrive at an improved interpretation scheme for the ball rebound screening test for viscoelastic loss. We begin with the analytical method of one-dimensional impact of a rigid object upon a viscoelastic layer, which is followed by more complex cases for which numerical techniques are required.

ONE-DIMENSIONAL ELASTIC BUFFER

The massless, linearly elastic block buffer in one dimension is mechanically equivalent to a spring. Consider, therefore, a one-dimensional mass–spring system. The mass m vibrates so that its displacement is

$$U(t) = A \sin (\omega_0 t + \theta), \tag{1}$$

in which $\omega_0 = \sqrt{(Ebc/mh)}$, E is the axial modulus of the elastic block, b and c are its cross-section dimensions, h is its axial length and A and θ are amplitude and phase constants, respectively, depending on the initial displacement and velocity of m.

Consider the impact of a mass m moving at velocity V on a spring. Equation (1) describes the motion of m following its contact with the spring at time $t = 0$. The dis-placement U of m is therefore

$$U(t) = \frac{V}{\omega_0} \sin (\omega_0 t) \tag{2}$$

and the impact force F is obtained to be

$$F(t) = m\omega_0 V \sin(\omega_0 t).\tag{3}$$

The impact force is linearly proportional to the deflection of the spring, or the displacement of m. The maximum impact force $F_{max} = V\sqrt{(mEbc/h)}$ for a maximum spring deflection $U_{max} = V\sqrt{(mh/Ebc)}$ at $t = \pi\sqrt{(mh/Ebc)}/2$. F_{max} is related to U_{max} by

$$F_{max} = \frac{Ebc}{h} U_{max}\tag{4}$$

and

$$F_{max} = Ebc\varepsilon,\tag{5}$$

in which ε is the maximum compressive engineering strain of the spring. Providing the maximum spring deflection is constrained, the minimum impact force is obtained with the smallest value of E. A value of

$$E = \frac{mV^2}{bch\varepsilon^2}\tag{6}$$

is the optimal stiffness to minimize F_{max}.

ONE-DIMENSIONAL VISCOELASTIC BUFFER BASED ON FREE DECAY OSCILLATION

Consider the one-dimensional mass–viscoelastic buffer system. In order to investigate the impact behavior in terms of the viscoelastic properties of the buffer directly, we approximate the impact as one half cycle of free decay oscillation. The governing equation for the one-dimensional forced oscillation of a linearly viscoelastic block with an attached mass m is similar to that given by Christensen (1982) for the torsional case, and is as follows:

$$F_{ext}(t) - U(t)bc\rho\omega^2 h \frac{\cot(\Omega^*)}{\Omega^*} = m\frac{\partial^2 U(t)}{\partial t^2},\tag{7}$$

in which $F_{ext}(t)$ is the external force $[F_{ext}(t) = F_0 \sin(\omega t)]$, $U(t)$ is the displacement of the mass m, b and c are the cross-section dimensions of the viscoelastic buffer, h is its axial length, ρ is its mass density, ω is the angular frequency of harmonic oscillation, $E^*(i\omega)$ or $E'(i\omega)[1 + i \tan \delta]$ is the uniaxial complex modulus, $E'(i\omega)$ is the storage modulus, $\tan \delta$ is the loss tangent, and $\Omega^* = \sqrt{(\rho\omega^2 h^2/E^*(i\omega))}$. The lateral restrictions at the ends of the buffer are neglected in eqn (7). This is considered appropriate since the analysis is on the basis of a one-dimensional problem. Physically, the one-dimensional approximation is appropriate for a stiff, flat-ended column, for a ribbed buffer composed of a series of such columns, or for perfectly lubricated compression of a block.

Now suppose the mass of the buffer is much less than that of the impactor as a result of a small density ρ or axial length h. Then we can approximate $\Omega^* \to 0$, and therefore $\cot(\Omega^*) \to 1/\Omega^*$. The buffer is therefore a massless viscoelastic spring and the induced deflection and stress are uniform in the axial direction. Equation (7) then yields

$$F_{ext}(t) - U(t)E^*(i\omega)\frac{bc}{h} = m\frac{\partial^2 U(t)}{\partial t^2}.\tag{8}$$

The external force $F(t)$ vanishes in the situation when the mass has struck the buffer and is vibrating freely upon it. The impact, from contact to peak force, is one quarter of a

cycle. The solution is then of the form

$$U(t) = A\, e^{\omega_0(-\alpha + i\beta)t - \theta i},$$ (9)

in which

$$\omega_0 = \sqrt{(E'(i\omega)bc/mh)}; \quad \alpha = (1 + \tan \delta^2)^{1/4} \sin(\delta/2); \quad \beta = (1 + \tan \delta^2)^{1/4} \cos(\delta/2);$$

and A and θ are constants depending on the initial displacement and velocity of m. This solution for free vibration of the mass–viscoelastic buffer system is identical to that for one-dimensional impact of mass m on a viscoelastic buffer. Based on the initial condition the displacement of m can be written

$$U(t) = \frac{V}{\beta\omega_0} \sin(\beta\omega_0 t)\, e^{-\alpha\omega_0 t},$$ (10)

in which V is the initial velocity of moving mass m, and the contact of m and the buffer again occurs at time $t = 0$.

Accordingly, the force induced on m is

$$F(t) = m\frac{\mathrm{d}^2 U(t)}{\mathrm{d}t^2}$$

$$= \frac{mV}{\beta}\omega_0[\beta^2 \sin(\beta\omega_0 t) + 2\alpha\beta \cos(\beta\omega_0 t) - \alpha^2 \sin(\beta\omega_0 t)]\, e^{-\alpha\omega_0 t}.$$ (11)

By equating $\mathrm{d}U(t)/\mathrm{d}t$ and $\mathrm{d}F(t)/\mathrm{d}t$ to zeros, respectively, the maximum displacement U_{max} and the maximum impact force F_{max} are derived in terms of the design parameters as

$$U_{max} = V\sqrt{\left(\frac{mh}{E'(i\omega)bc}\right)}\frac{1}{(1 + \tan \delta^2)^{1/4}}\, e^{-\tan(\delta/2)(\pi/2 - \delta/2)}$$ (12)

at

$$t = \frac{\pi - \delta}{2(1 + \tan \delta^2)^{1/4} \cos\left(\dfrac{\delta}{2}\right)\omega_0},$$

and

$$F_{max} = V\sqrt{\left(\frac{mE'(i\omega)bc}{h}\right)}(1 + \tan \delta^2)^{1/4}\, e^{-\tan(\delta/2)(\pi/2 - 3\delta/2)}$$ (13)

at

$$t = \frac{\pi - 3\delta}{2(1 + \tan \delta^2)^{1/4} \cos\left(\dfrac{\delta}{2}\right)\omega_0}$$

for $\tan \delta \leqslant 1.73$, or

$$F_{max} = 2V\sqrt{\left(\frac{mE'(i\omega)bc}{h}\right)}(1 + \tan \delta^2)^{1/4} \sin\left(\frac{\delta}{2}\right)$$ (14)

at $t = 0$, for $\tan \delta \geqslant 1.73$.

It can be determined from eqn (12) that

$$E'(i\omega) = \frac{mV^2h}{bc}\left(\frac{1}{U_{max}}\right)^2 \frac{1}{(1+\tan\delta^2)^{1/2}}\, e^{-\tan(\delta/2)(\pi-\delta)} \tag{15}$$

is the optimal stiffness if there is a limit U_{max} on the maximum deflection. Substituting eqn (15) in eqns (13) and (14), F_{max} can be obtained to be

$$F_{max} = \frac{mV^2}{U_{max}}\, e^{-\tan(\delta/2)(\pi-2\delta)} \tag{16}$$

for $\tan\delta \leqslant 1.73$, or

$$F_{max} = 2\frac{mV^2}{U_{max}} \sin\left(\frac{\delta}{2}\right) e^{-\tan(\delta/2)(\pi/2-\delta/2)} \tag{17}$$

for $\tan\delta \geqslant 1.73$. Differentiating eqns (13) and (16) with respect to δ, the optimal loss tangent $\tan\delta$ to minimize the impact force is determined to be 0.4 if the stiffness is held constant and 1.1 if the stiffness is treated as a design variable. For $\tan\delta = 1.1$ the optimal value of $E'(i\omega)$ is 24% of the value for the optimized elastic buffer, based on eqn (15). The resulting impact force is 52% of the value found in the optimized elastic buffer, based on eqn (16).

As in the elastic case, U_{max}, F_{max} and the optimal $E'(i\omega)$ of the viscoelastic buffer are proportional to the values of $V\sqrt{(mh/(E'(i\omega)bc))}$, $V\sqrt{(mE'(i\omega)bc/h)}$ and $mV^2/(bch\varepsilon^2)$, which are basically dependent on the design parameters.

Numerical values are assumed to provide numerical examples. An adaptation of the values quoted by Burton (1984) for assessment of artificial sports surfaces is used. The values are $b = c = 150$ mm; $h = 50$ mm; $m = 5400$ g; $V = 6.26$ m s^{-1} (assume mass is dropped from a height of 2 m). This was orginally a hollow metal ball with an accelerometer inside. The approximation cot $(\Omega^*) \rightarrow 1/\Omega^*$ which was required to obtain the solutions was checked with these values. It was found that the differences between both real and imaginary parts of cot (Ω^*) and $1/\Omega^*$ are within 10%. Results are shown in the following figures. First, the loss tangent was varied and the stiffness of the material was adjusted so that the maximum compression of the buffer was always 50%. Force vs deflection curves for different loss tangents are given in Fig. 1. The maximum force F_{max} vs tan δ curve obtained from eqns (16) and (17), as shown in Fig. 2, shows that the peak impact force is the smallest when $\tan\delta \cong 1$. If, however, the material stiffness E' is kept constant, the maximum compressive strain ε in the buffer during impact will decrease when the loss tangent of the buffer increases. The impact force then becomes large for high values of the buffer loss tangent, as is also shown in Fig. 2. As in the case of an elastic buffer, to minimize the impact force, the thickness h is to be maximized. Equations (13) and (14) imply that F_{max} is proportional to the inverse of the square root of h. For example, a 50% increase in thickness results in an 18% decrease in peak force.

With the solutions of $U(t)$ and $F(t)$ given above, tan δ of viscoelastic materials can be determined from the coefficient of restitution extracted from the one-dimensional rebound test. A mass dropped from height H_0 on the tested materials at $t = 0$ rebounds back with velocity V_1 at time t_{cont} and back to height H_1. The contact time t_{cont} is obtained by equating $F(t)$ to zero

$$t_{cont} = \frac{\pi-\delta}{(1+\tan\delta^2)^{1/4}\cos\left(\frac{\delta}{2}\right)\omega_0} \tag{18}$$
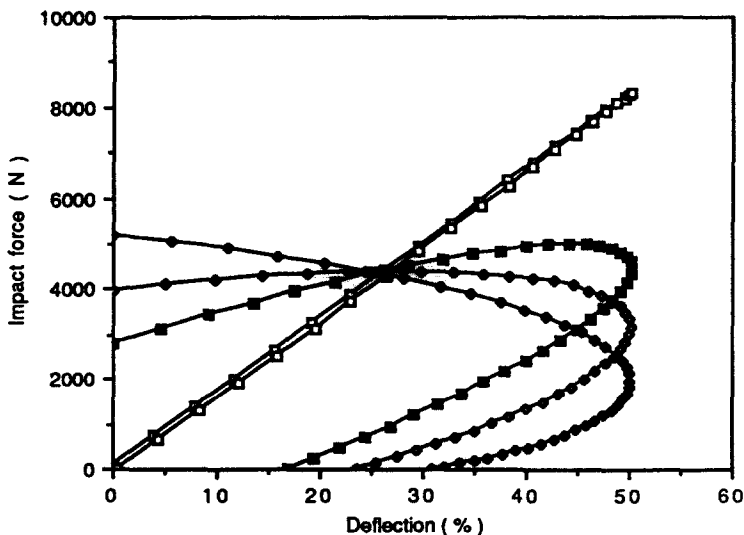
with $\omega_0 = \sqrt{(Ebc/mh)}$.

Fig. 1. Impact force vs deflection curves for different loss tangents, one-dimensional viscoelastic buffer based on free decay oscillation, E' adjusted so as to obtain $\varepsilon = 50\%$. □: $\tan \delta = 0.01$; ■: $\tan \delta = 0.5$; ◇: $\tan \delta = 1$; ◆: $\tan \delta = 5$.
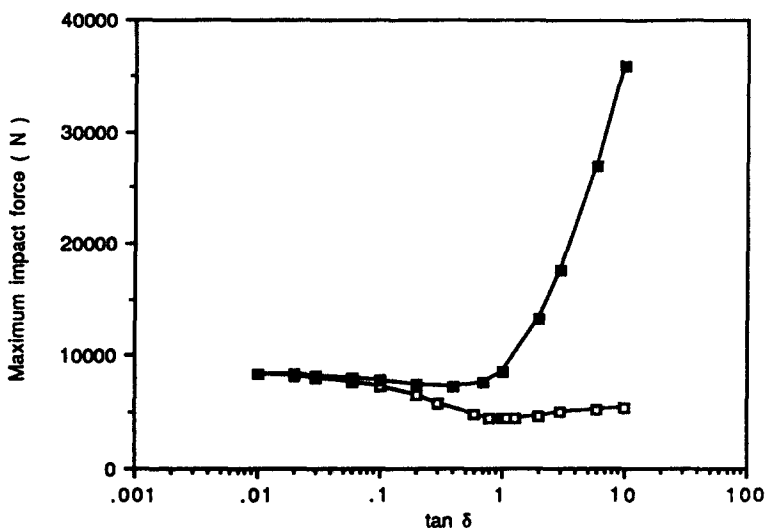

Fig. 2. Maximum impact force of one-dimensional viscoelastic buffer based on free decay oscillation. □: E' adjusted so as to obtain the maximum compressive strain $\varepsilon = 50\%$; ■: $E' = 0.75$ MPa, ε varied.

V_1 is obtained by substituting t_{cont} in the time derivative of $U(t)$. Tan δ is therefore related to H_0 and H_1 by

$$\frac{H_1}{H_0} = \left(\cos \delta + \tan \frac{\delta}{2} \sin \delta \right) e^{-2 \tan (\delta/2)(\pi - \delta)} \tag{19}$$

If $\tan \delta$ is small, the relation above can be approximated to be

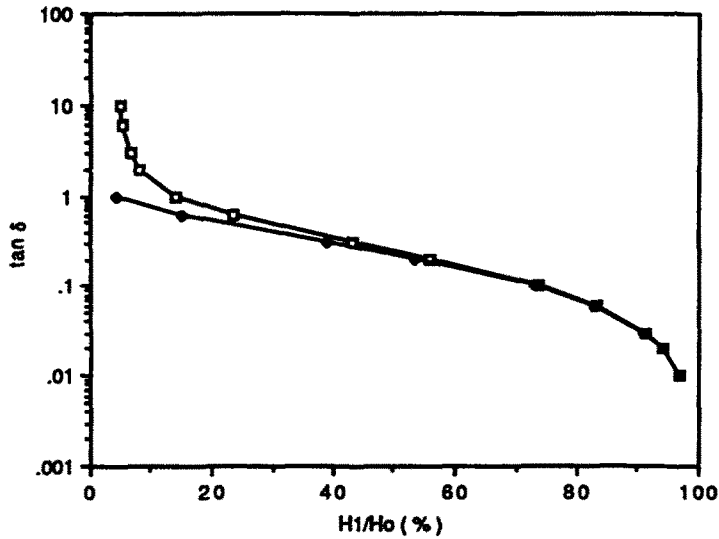$$\tan \delta \cong \frac{\ln \left(\dfrac{H_0}{H_1} \right)}{\pi} \tag{20}$$

Fig. 3. Tan δ obtained from the ball rebound test. $\square$: exact value by one-dimensional viscoelastic buffer based on free decay oscillation; $\blacklozenge$: approximated by tan $\delta \cong \ln (H_0/H_1)/\pi$.

Figure 3 shows the analytical prediction of tan δ from assumed rebound height ratios $H_1 H_0$. The much simpler approximation formula of eqn (20) is applicable for tan $\delta \leqslant 0.2$. This form is the one quoted by Flom (1960) and Calvit (1967); it is an *approximation* valid for small loss.

ONE-DIMENSIONAL VISCOELASTIC BUFFER WITH THE TRANSIENT TERM CONSIDERED

For the problems considered in the previous section, the starting transients were neglected during the impact such that in the analysis only free decay terms were considered. The same problems will now be analyzed with the transient starting effects due to the viscoelasticity of the buffer material included. An integral transform method is used for obtaining solutions.

For the sake of simplicity and feasibility, the solutions are obtained for a linearly viscoelastic material represented by a three-element model described by the first two terms of the generalized Maxwell model,

$$E(t) = E_0 + E_1 e^{-t/t_1} + E_2 e^{-t/t_2} + \cdots + E_n e^{-t/t_n}.$$

It is necessary in this case to assume a particular type of material since the transient contains a distribution of frequencies. Consequently, tan δ over a range of frequencies will contribute. The relaxation function, the storage modulus, and the loss tangent are given by

$$E(t) = E_0 + E_1 e^{-t/t_1} \tag{21}$$

$$E'(\omega) = E_0 + E_1 \frac{\omega^2}{\left(\omega^2 + \dfrac{1}{t_1^2}\right)} \tag{22}$$

and

$$\tan \delta(\omega) = \omega \frac{E_1}{t_1(E_0 + E_1)\omega^2 + E_0 \dfrac{1}{t_1^2}}, \tag{23}$$

in which ω is the frequency of harmonic oscillation. E' and $\tan \delta$ are functions of ω. Equations (21)–(23) represent a single discrete relaxation time in the spectrum. In this model, the values of E_0, E_1, and t_1 were adjusted to obtain the desired value of $\tan \delta$ at the principal frequency associated with the impact. This frequency was derived from the contact time between the mass and the buffer. In view of this procedure, the single spectral line chosen is the most significant one in the spectrum.

For a one-dimensional impact, Newton's second law applied to a viscoelastic material is given by

$$m\frac{\mathrm{d}^2 U(t)}{\mathrm{d}t^2} = -\frac{bc}{h}\int_0^t E(t-\tau)\frac{\mathrm{d}U(\tau)}{\mathrm{d}\tau}\mathrm{d}\tau. \tag{24}$$

Taking the Laplace transformation of eqn (24) with the same initial conditions as applied in the previous sections, we can obtain the Laplace transformation form

$$[U(s)] = \frac{P(s)}{Q(s)}$$

$$= \frac{V\left(s+\dfrac{1}{t_1}\right)}{s^3+\dfrac{1}{t_1}s^2+\dfrac{bc(E_0+E_1)}{hm}s+\dfrac{bcE_0}{hm}}. \tag{25}$$

The inverse transformation of eqn (25) yields the solution

$$U(t) = V\{k_1 \, e^{z_0 t}+k_2 \, e^{x_1 t} \, (k_3 \sin (\beta_1 t)+k_4 \cos (\beta_1 t))\}, \tag{26}$$

which is a decaying sinusoidal function for low loss materials, or

$$U(t) = V\{k_5 \, e^{z_0 t}+k_6 \, e^{z_1 t}+k_7 \, e^{z_2 t}\}, \tag{27}$$

which is a decaying exponential function for high loss materials. In these expressions, V is the initial velocity of the moving mass m; z_0, $\alpha_1+i\beta_1$ and $\alpha_1-i\beta_1$ or z_0, z_1 and z_2 are roots of the third order polynomial equation $Q(s)$ and are obtained numerically; k_1, k_2, k_3, and k_4 are functions of t_1, z_0, α_1 and β_1; and k_5, k_6 and k_7 are functions of t_1, z_0, z_1 and z_2.

Accordingly, the impact force is obtained as

$$F(t) = -m\frac{\mathrm{d}^2 U(t)}{\mathrm{d}t^2}$$

$$= -mV\{z_0^2 k_1 \, e^{z_0 t}+k_2\alpha_1^2 \, e^{x_1 t} \, (k_3 \sin (\beta_1 t)+k_4 \cos (\beta_1 t))+2k_2\alpha_1\beta_1 \, e^{x_1 t} \, (k_3 \cos (\beta_1 t)$$

$$-k_4 \sin (\beta_1 t))+k_2\beta_1^2 \, e^{x_1 t} \, (-k_3 \sin (\beta_1 t)-k_4 \cos (\beta_1 t))\} \tag{28}$$

from eqn (26), or

$$F(t) = -mV\{z_0^2 k_5 \, e^{z_0 t}+z_1^2 k_6 \, e^{z_1 t}+z_2^2 k_7 \, e^{z_2 t}\} \tag{29}$$

from eqn (27).

We now reconsider the problem as an elastic case. Equation (24) will reduce directly to

$$m\frac{\mathrm{d}^2 U(t)}{\mathrm{d}t^2} = -\frac{EbcU(t)}{h}, \tag{30}$$

which is exactly the same as obtained in the previous section. It is important to observe

that the starting transients only exist in the viscoelastic case and therefore the behavior of the elastic buffer is just the same as described before.

The relations between the design parameters and U_{max} and F_{max} are no longer expressed explicitly. Consequently, a numerical method is used to obtain the solutions. Numerical examples are investigated with the same parameters as before.

The stiffness and the loss tangent of the material are simultaneously varied to obtain a 50% compressive deformation of the buffer. Force vs deflection curves for different loss tangents obtained by this analysis are given in Fig. 4. Regardless of the value of tan δ, the impact force always vanishes at $t = 0$. However, the peak of impact force occurs at an earlier time when tan δ increases. The maximum impact force is minimized when tan δ is 1-2 if the maximum compressive strain ε is held at 50%, as shown in Fig. 5. The effect of the transient term is as follows. With the transient included, the optimal material properties are tan $\delta \cong 1$ and a stiffness E' which is 35% of the value for the best elastic buffer; the peak impact force F_{max} is 69% of that for the elastic buffer. The solution neglecting the
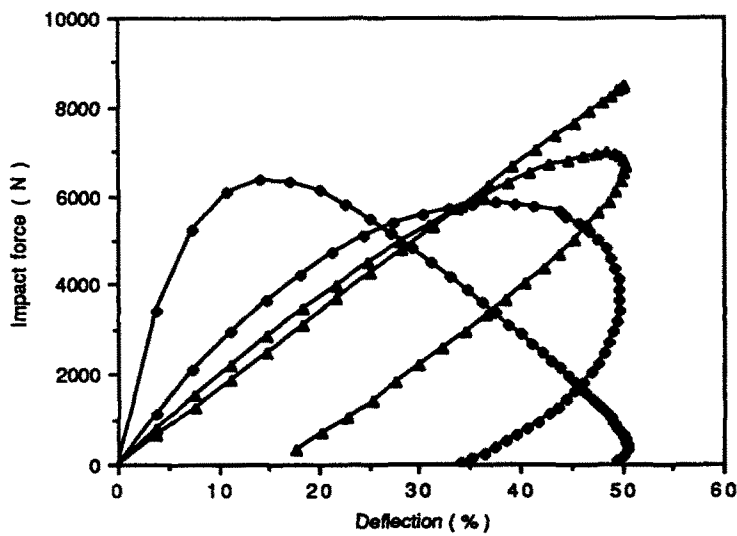
Fig. 4. Impact force vs deflection curves for different loss tangents, one-dimensional viscoelastic buffer with the transient term considered, E' adjusted so as to obtain $\varepsilon = 50\%$. $\triangle$: elastic; $\blacktriangle$: tan $\delta = 0.34$; $\diamondsuit$: tan $\delta = 1$; $\blacklozenge$: tan $\delta = 7$.
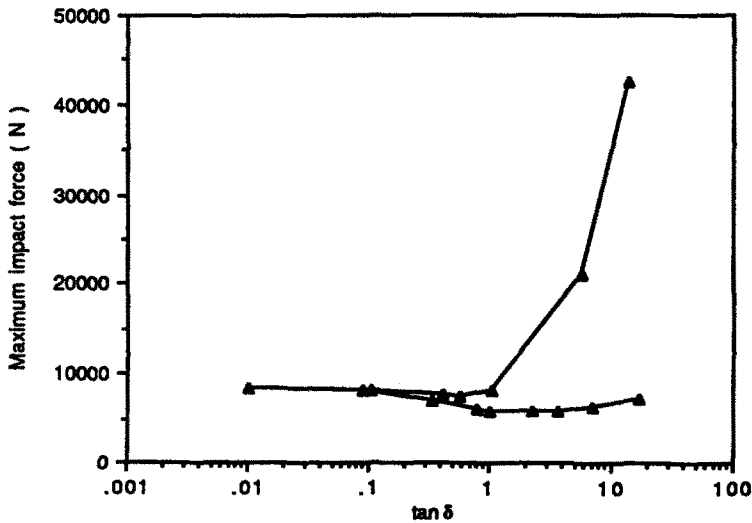
Fig. 5. Maximum impact force of one-dimensional viscoelastic buffer with the transient term considered. $\triangle$: E' adjusted so as to obtain the maximum compressive strain, $\varepsilon = 50\%$; $\blacktriangle$: $E' = 0.75$ MPa, ε varied.
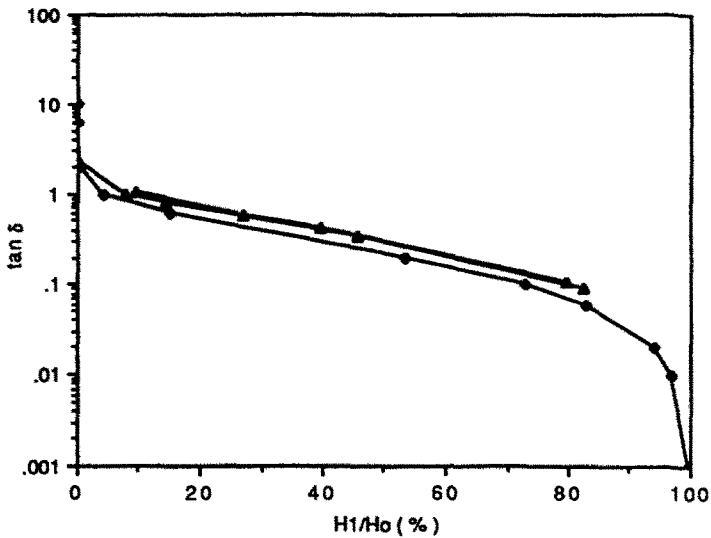
Fig. 6. Tan δ obtained from the ball rebound test. $\triangle$: exact value by one-dimensional viscoelastic buffer with the transient term considered, E' adjusted so as to obtain $\varepsilon = 50\%$; $\blacktriangle$: $E' = 0.75$ MPa. ε varied; $\blacklozenge$: approximated by tan $\delta \cong \ln (H_0/H_1)/\pi$.

transient also results in tan $\delta = 1$, but E' is 24% of that of the elastic buffer and the peak force is 52% of that for the elastic buffer. Therefore, neglect of the transient leads to an overly optimistic design. The impact force is recalculated assuming no variation in the stiffness E'. This gives a shallower minimum in the force vs loss curve, and a substantial increase in force for large loss. This comparison, also shown in Fig. 5, is similar to that in Fig. 2, which was obtained by a more simple analysis.

As for the rebound test, the relation between tan δ and the rebound height ratio H_1/H_0 according to the present analysis is given in Fig. 6. Observe that the simple approximation formula underestimates the loss tangent.

IMPACT OF A RIGID SPHERE ONTO A VISCOELASTIC HALF-SPACE

Earlier analyses were given for spatially one-dimensional solutions of impact of a mass upon a viscoelastic buffer of finite thickness. As an extension of viscoelastic impact problems, the penetration of a viscoelastic half-space by a rigid spherical indenter is investigated. The purpose is to evaluate the effect of the spatially nonuniform stress distribution and its time evolution upon the viscoelastic impact. However, for the design consideration, the width and thickness of the buffer must be sufficiently large that the penetration of the indenter onto the buffer is limited to a local area since the buffer is now assumed to be a half-space. Again, the viscoelastic behavior is simplified to be a standard linear solid with a single relaxation time as in the previous section. Therefore, the transient term is also included.

If a ball of mass m and radius R is dropped onto a viscoelastic half-space whose relaxation and creep functions in shear are given by $G(t)$ and $J(t)$, respectively, the governing equations are given by Hunter (1960) as

$$m\frac{d^2 U(t)}{dt^2} = \frac{-8R^{1/2}}{3(1-v)} \int_0^t G(t-\tau)\, d(U^{3/2}(\tau)) \tag{31}$$

and

$$U(t) = \frac{r^2(t)}{R} \tag{32}$$

when the ball loads $(0 \leqslant t \leqslant t_m)$, and

$$m \frac{d^2 U(t)}{dt^2} = \frac{-8}{3(1-v)R} \int_0^{t_r(t)} G(t-\tau) \, d(r^3(\tau)) \qquad (33)$$

and

$$U(t) = \frac{r^2(t)}{R} - \frac{1}{R} \int_{t_m}^t J(t-t') \frac{d \int_{t_r(t')}^{t'} G(t'-\tau) \frac{dr^2(\tau)}{d\tau} \, d\tau}{dt'} \, dt' \qquad (34)$$

when the ball rebounds $(t_m \leqslant t)$, in which v is Poisson's ratio and is considered to be 0.3, constant in time, $r(t)$ is the radius of contact area, t_m is the time at which both $U(t)$ and $r(t)$ reach the maximum values, and $r(t_r(t)) = r(t)$ for $0 \leqslant t_r(t) \leqslant t_m$, and $t_m < t$.

First start with the elastic solutions. Equation (31) is replaced by

$$F(t) = -m \frac{d^2 U(t)}{dt^2}$$

$$= \frac{8R^{1/2} G U^{(3/2)}(t)}{3(1-v)}, \qquad (35)$$

in which G is the elastic shear modulus. Integrating eqn (35), the displacement of the ball $U(t)$ is obtained to be

$$U(t) = \left(\frac{15}{32}\right)^{2/5} \frac{(1-v)^{2/5} m^{2/5} (V^2 - (dU(t)/dt)^2)^{2/5}}{R^{1/5} G^{2/5}}, \qquad (36)$$

in which V is the initial velocity of m. Equating $dU(t)/dt$ to zero at $t = t_m$, the maximum displacement U_{max} and the maximum impact force F_{max} are determined to be

$$U_{max} = \left(\frac{15}{32}\right)^{2/5} \frac{(1-v)^{2/5} m^{2/5} V^{4/5}}{R^{1/5} G^{2/5}} \qquad (37)$$

and

$$F_{max} = \frac{8R^{1/2} G U_{max}^{3/2}}{3(1-v)}$$

$$= \left(\frac{15}{32}\right)^{3/5} \frac{8 m^{3/5} V^{6/5} R^{1/5} G^{2/5}}{3(1-v)^{2/5}}, \qquad (38)$$

respectively. It is clear that $G = (15/32)(1-v)mV^2/(R^{1/5}(U_{max})^{5/2})$ will minimize the impact force if there is an upper bound on U_{max}.

Now consider the viscoelastic case. For $0 \leqslant t \leqslant t_m$, performing a Laplace transform and its inverse transform on eqn (31), with $G(t)$ replaced by $G_0 + G_1 e^{-t/t_1}$, gives

$$\frac{d^3 U(t)}{dt^3} + \frac{1}{t_1} \frac{d^2 U(t)}{dt^2} + \frac{4R^{1/2}}{(1-v)m} (G_0 + G_1) U^{1/2}(t) \frac{dU(t)}{dt} + \frac{8R^{1/2} G_0}{3(1-v)mt_1} U^{3/2}(t) = 0. \quad (39)$$

Equation (39) can be solved using a single-step Euler method to the third order differentiation of $U(t)$. The accuracy of the Euler method depends on the mesh width H in the forward difference integration. An elastic impact problem described by the

ordinary differential eqn (36) was solved analytically to check on the sensitivity of the Euler method to the mesh width H. It was found that good agreement was obtained when $H = 0.00001$ s. It should be pointed out that no effort was made to seek the generally optimal time interval for the numerical method. $H = 0.00001$ s was thus used in this analysis for convenience.

Solutions for eqns (33) and (34), which are the governing equations of ball rebound for $t_m \leqslant t$, are more complicated. To apply the numerical method, we first seek a means to break up the term with the double integral and derivatives in eqn (34). Following integration by parts, eqns (34) and (33) become

$$U(t) = \frac{r^2(t)}{R} - \frac{1}{R} \left\{ G_0 J_1 (1 - e^{(-t + t_r(t))/t_1}) r^2(t) - G_0 \frac{J_1}{t_1} e^{-t/t_1} \int_{t_r(t)}^{t} e^{\tau/t_1} r^2(\tau) \, d\tau \right.$$

$$+ G_1 \frac{J_1}{t_2} e^{-t/t_2} \int_{t_m}^{t} e^{\tau/t_2} (1 - e^{(-\tau + t_r(\tau))/t_1}) r^2(\tau) \, d\tau$$

$$\left. - G_1 \frac{J_1}{t_1 t_2} e^{-t/t_2} \int_{t_m}^{t} e^{t'/t_2} e^{t'/t_1} \int_{t_r(t')}^{t'} e^{\tau/t_1} r^2(\tau) \, d\tau \, dt' \right\}, \quad (40)$$

in which $J_1 = G_1/(G_0(G_0 + G_1))$ and $t_2 = G_0/(t_1(G_0 + G_1))$ with $J(t) = 1/G_0 - J_1 e^{-t/t_2}$, and

$$\frac{d^2 U(t)}{dt^2} = \frac{-8}{3(1 - v)mR} \left\{ G_0 r^3(t) + G_1 e^{(-t + t_r(t))/t_1} r^3(t) - \frac{G_1}{t_1} e^{-t/t_1} \int_0^{t_r(t)} e^{\tau/t_1} r^3(\tau) \, d\tau \right\}. \quad (41)$$

It is clear that $U(t)$ cannot be solved explicitly since the unknown function $t_r(t)$ is involved. However, a solution can be obtained by an iteration process as described by Calvit (1967). The solutions can be obtained to any time $t > t_m$ up to the point where the ball separates from the viscoelastic half-space.

Numerical values adapted from Burton (1984) are again assumed in order to investigate the behavior of the impact system. However, the hollow indenter of $m = 5400$ g and $R = 110$ mm is dropped from a lower height of 200 mm to result in a small deformation as required. Curves of force vs deflection and radius of contact vs deflection are shown in Figs 7 and 8, respectively. It is worth mentioning that the indenter has the same contact radius $r(t)$ at a
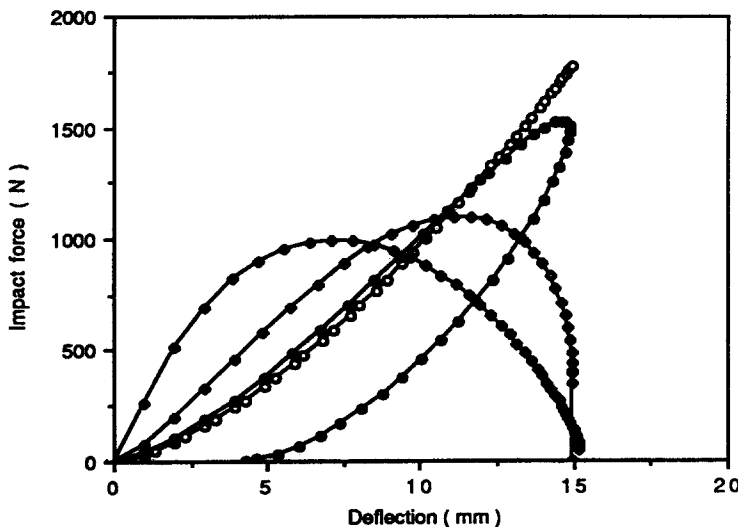

Fig. 7. Impact force vs deflection curves for different loss tangents, a rigid sphere onto a viscoelastic half-space, G' adjusted so as to obtain $U_{max} = 15$ mm. $\bigcirc$: elastic; $\bullet$: tan $\delta = 0.33$; $\diamond$: tan $\delta = 2.3$; $\blacklozenge$: tan $\delta = 10$.
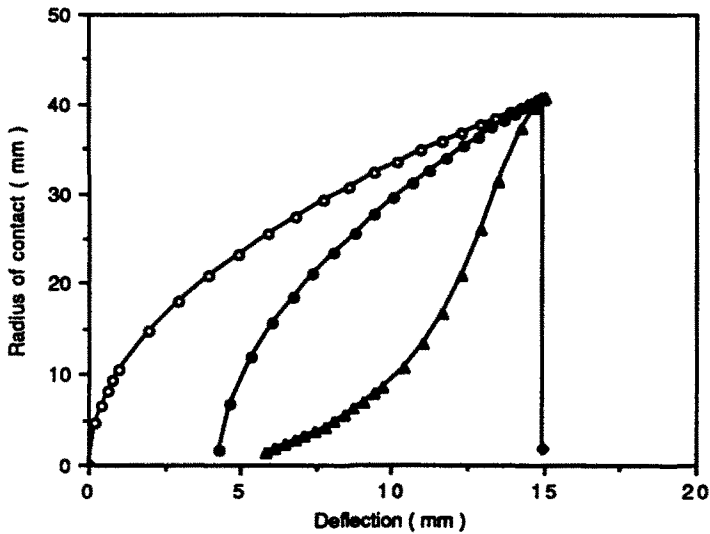
Fig. 8. Radius of contact between the rigid sphere and a viscoelastic half-space of different loss tangents. $\bigcirc$: loading curve of different loss tangent half-space and rebound curve for elastic half-space; $\bullet$: rebound curve; $\tan \delta = 0.33$; $\triangle$: $\tan \delta = 0.87$; $\diamondsuit$: $\tan \delta \geqslant 2.3$.

certain $U(t)$ for elastic and viscoelastic half-spaces during the loading, and a smaller $r(t)$ for a higher loss half-space during the rebounding.

As shown in Fig. 9, the peak impact force reaches a minimum value when $\tan \delta$ is 1-2 if G' is kept at 0.77 MPa and $\tan \delta$ is varied. The peak impact force becomes small for high values of $\tan \delta$ up to 10 if G' is adjusted so that the maximum deflection is always 15 mm. The optimal values of G' are found to be 48 and 4% of the value of the optimal elastic half-space for $\tan \delta$ equal to 1 and 10, respectively. However, it is worth noting that the contact area varies during the impact. A small peak force still means a high stress level over the contact area when $\tan \delta$ is large. Figure 10 shows the comparisons between $R = 110$ mm and $R = 60$ mm when G' is kept constant at 0.77 MPa. The peak impact force decreases if the radius of the ball decreases. In any case, a smaller ball will cause a larger value of maximum deflection.
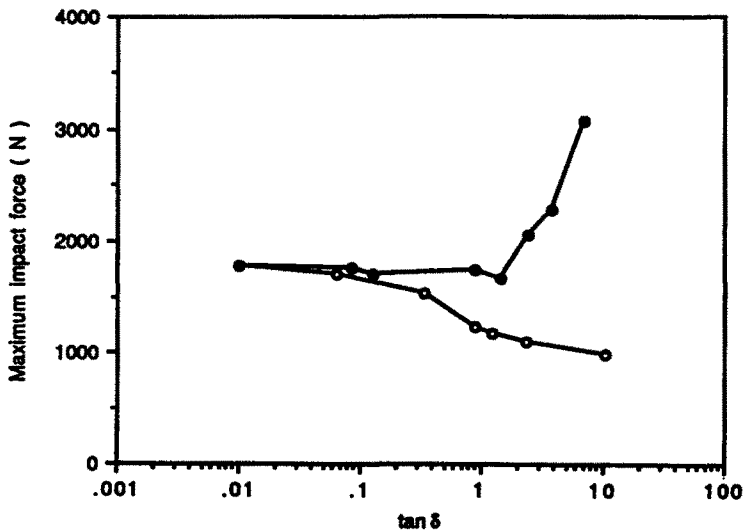

Fig. 9. Maximum impact force of a rigid sphere onto a viscoelastic half-space. $\bigcirc$: G' adjusted so as to obtain $U_{max} = 15$ mm; $\bullet$: $G' = 0.77$ MPa, U_{max} varied.
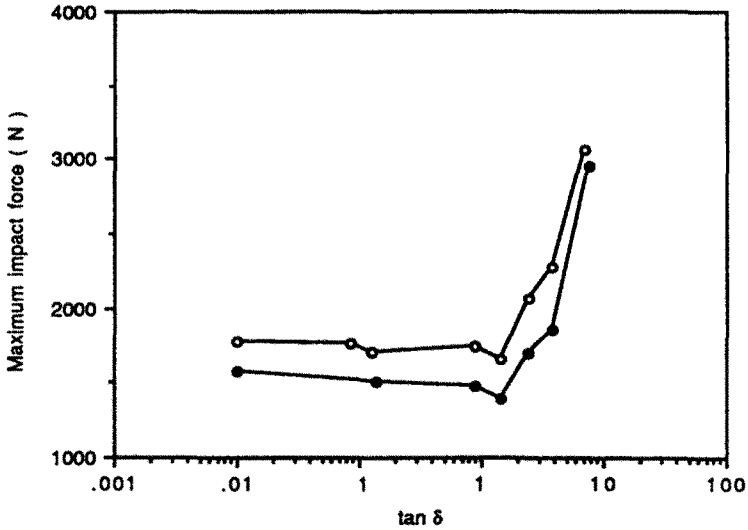
Fig. 10. Maximum impact force of a rigid sphere onto a viscoelastic half-space, $G' = 0.77$ MPa, U_{max} varied. $\bigcirc$: radius of the sphere $R = 110$ mm; $\bullet$: $R = 60$ mm.
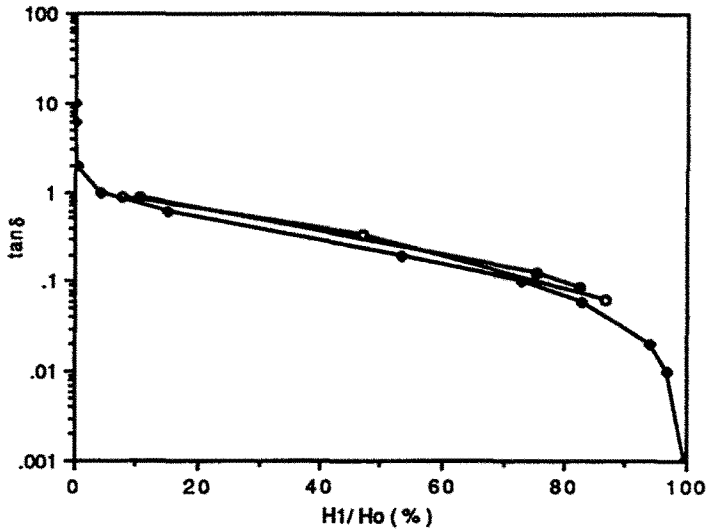

Fig. 11. Tan δ obtained from the ball rebound test. $\bigcirc$: exact value by a rigid sphere onto a viscoelastic half-space, G' adjusted so as to obtain $U_{max} = 15$ mm; $\bullet$: $G' = 0.77$ MPa, U_{max} varied; $\blacklozenge$: approximated by tan $\delta \cong \ln (H_0/H_1)/\pi$.

As for the analysis of the ball rebound test, the loss tangent predicted from the coefficient of restitution is somewhat greater than that from the elementary formula, eqn (20), as shown in Fig. 11.

A synopsis of the results for different assumed conditions is given in Fig. 12 for impact force, and in Fig. 13 for rebound restitution vs loss tangent.

DISCUSSION

The application of linearly viscoelastic materials to the reduction of impact force has been considered. Solution of the material design problem for a one-dimensional flat-ended impactor yields an optimum loss tangent of approximately one. Loss tangents of this magnitude are available in a variety of polymers as described by Ferry (1970). Elastomers with high loss over frequencies from 10 to 1000 Hz were characterized by Shipkowitz *et al.* (1988). We therefore view the optimal material properties as physically realizable. If material
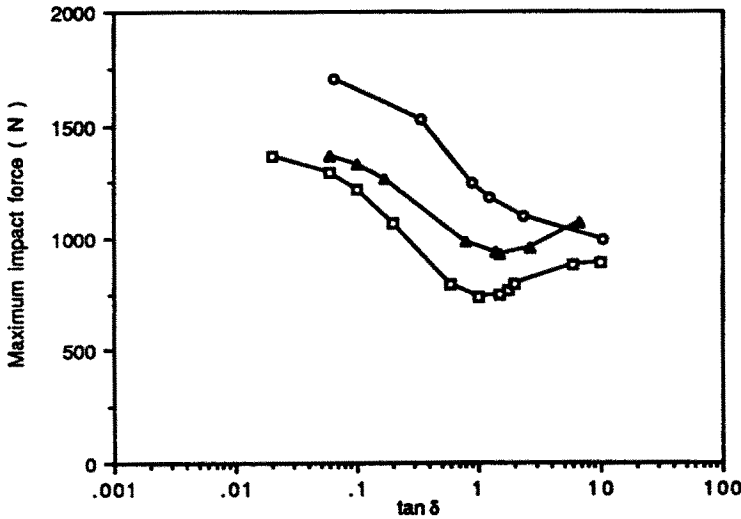
Fig. 12. Comparison of maximum impact force obtained from different considerations, ball dropped from a height of 200 mm. $\bigcirc$: spherical indenter, G' varied, $U_{max} = 15$ mm; $\square$: one-dimensional, free decay oscillation, E' varied, $U_{max} = 15$ mm; $\triangle$: one-dimensional, with transient term, E' varied, $U_{max} = 15$ mm.

Fig. 13. Tan δ obtained from different considerations, ball dropped from a height of 200 mm. $\bigcirc$: spherical indenter, G' varied, $U_{max} = 15$ mm; $\square$: one-dimensional, free decay oscillation, E' varied, $U_{max} = 15$ mm; $\triangle$: one-dime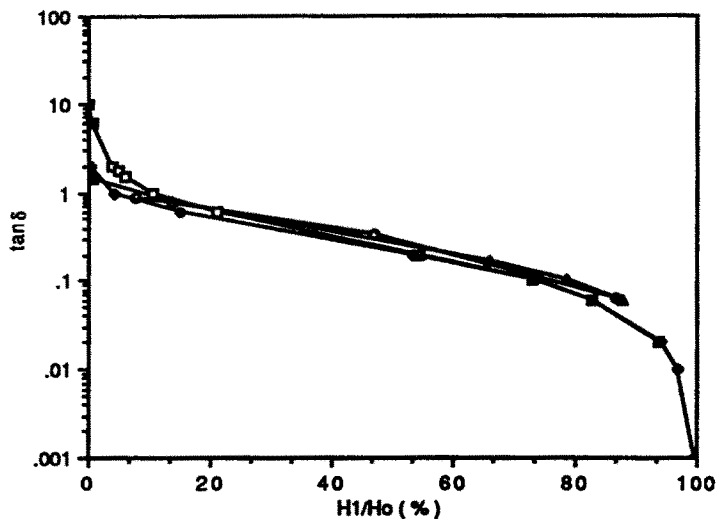nsional, with transient term, E' varied, $U_{max} = 15$ mm; $\blacklozenge$: approximated by tan $\delta \cong \ln (H_0/H_1)/\pi$.

stiffness as E' is also included as a design variable, the optimum stiffness is less than that of an elastic buffer by a factor of three to four, and reductions in peak force approaching a factor of two are possible, in comparison with an elastic buffer of the same geometry. The conclusion is thus far independent of the degree of sophistication of the mathematical model, so that further refinements, such as inclusion of multiple relaxation peaks, are unlikely to be productive. In the case of a spherical indenter, the optimal loss tangent is considerably greater, of the order of 10. This difference is attributed to the geometrically nonlinear nature of this problem, as indicated by the fact that the force–displacement curve for an elastic material is concave up (Fig. 7). This type of nonlinearity is unfavorable from the point of view of minimizing the peak force for a given amount of energy (area under the curve). Consequently, more loss is needed than in the case of a flat indenter. By contrast, the material nonlinearity (which also has a geometrical cause) in foams is of the opposite

nature, as indicated by Gibson and Ashby (1988). The appropriate foam can also reduce impact force by a factor of nearly two. Foams have the advantage of light weight and the disadvantage of "bottoming out" under a force greater than the value designed for, as well as a rebound effect not seen in highly viscoelastic materials. However, viscoelastic materials of very high loss tend to be temperature sensitive. As for three-dimensional aspects, we observe that elastomers, whether they be highly viscoelastic or not, have a Poisson's ratio very close to 0.5. Consequently, a ribbed design is called for in the case of a thin buffer, to allow the material to expand laterally when squeezed. Finally, in the case of the ball rebound test, we remark that the test would be difficult to use for loss tangents exceeding two as a result of the extreme steepness of the curve in Fig. 11.

CONCLUSIONS

(1) For an elastic buffer, the impact force is minimized by a buffer which is as thick as possible and which has an appropriate Young's modulus.

(2) Impact force is minimized by a flat-surface viscoelastic buffer with a loss tangent near one.

(3) To achieve significant force reduction of a factor of two in comparison with an elastic material, the Young's modulus of the viscoelastic buffer must be smaller by a factor of about four than the optimum for an elastic buffer.

(4) The optimum material properties of the viscoelastic impact absorber depend upon the shape of the impactor. For a spherical indenter on a viscoelastic substrate, the impact force is minimized for a substrate with a loss tangent of 10 or greater and a stiffness smaller by a factor of about 25 in comparison with the elastic case.

(5) As for the ball rebound method for screening materials for viscoelastic loss, the formula given by Flom (1960) and Calvit (1967) is seen to be an approximation, valid for small loss. We present a more sophisticated interpretation scheme, valid for high loss materials.

REFERENCES

Burton, R. D. (1984). Physical properties of Sorbothane, 6. Determination of impact properties. BTR Industrial Ltd, Central Development, Burton-on-Trent, U.K.
Calvit, H. H. (1967). Numerical solution of the problem of impact of a rigid sphere onto a linear viscoelastic half-space and comparison with experiment. *Int. J. Solids Struct.* 3, 951–966.
Christensen, R. M. (1982). *Theory of Viscoelasticity*, 2nd Edn. Academic Press, New York.
Ferry, J. D. (1970). *Viscoelastic Properties of Polymers*. John Wiley, New York.
Flom, D. G. (1960). Rolling friction of polymeric materials. I. Elastomers. *J. Appl. Phys.* 31, 306–314.
Gibson, L. J. and Ashby, M. F. (1988). *Cellular Solids*. Pergamon Press, Oxford.
Hunter, S. C. (1960). The Hertz problem for a rigid spherical indenter and a viscoelastic half-space. *J. Mech. Solids* 8, 219–234.
Light, L. H., Mclellan, G. E. and Klenerman, L. (1980). Skeletal transients on heel strike in normal walking with different footwear. *J. Biomech.* 13, 477–480.
Pao, Y.-H. (1955). Extension of the Hertz theory of impact to the viscoelastic case. *J. Appl. Mech.* 26, 1083–1088.
Shipkowitz, A. T., Chen, C. P. and Lakes, R. S. (1988). Characterization of high-loss viscoelastic elastomers. *J. Mater. Sci.* 23, 3660–3665.
Tillett, J. P. A. (1954). A study of the impact on spheres of plates. *Proc. Lond. Phys. Soc.* 67, 677–688.
Voloshin, A. and Wosk, J. (1982). An *in vivo* study of low back pain and shock absorption in the human locomotor system. *J. Biomech.* 15, 21–27.
Zener, C. (1941). The intrinsic inelasticity of large plates. *Phys. Rev.* 59, 669–673.